



Catalytic valorization of bioethanol over Cu-Mg-Al mixed oxide catalysts

Ioan-Cezar Marcu¹, Didier Tichit, François Fajula, Nathalie Tanchoux^{*}

Institut Charles Gerhardt, UMR 5253 CNRS/ENSCM/UM2/UM1, Matériaux Avancés pour la Catalyse et la Santé (MACS), Ecole Nationale Supérieure de Chimie, 8, rue de l'Ecole Normale, 34296 Montpellier Cedex 5, France

ARTICLE INFO

Article history:

Received 14 April 2008

Received in revised form 9 April 2009

Accepted 10 April 2009

Available online 9 May 2009

Keywords:

Mixed oxide catalysts

Layered double hydroxides

Bioethanol

Butanol

Diethoxyethane

ABSTRACT

The conversion of ethanol into 1-butanol and 1,1-diethoxyethane was studied over Cu-Mg-Al mixed oxide catalysts obtained from LDH precursors. The optimum yields are obtained for Cu loadings comprised between 5 and 10 at.%. A reaction scheme accounting for the main and secondary reaction products is proposed. The influences of the reaction temperature and of the reaction time on the catalytic performances have also been investigated. The negative effect of water, a by-product of the reaction, on this transformation was evidenced.

© 2009 Elsevier B.V. All rights reserved.

1. Introduction

The demand for alternative renewable energy sources, particularly in the transportation sector, is ever growing. This sector is indeed at 96% dependent on non-renewable fossil fuels, and is responsible for the majority of petroleum-based greenhouse gas emissions. Alternative routes are then proposed for the production of biofuels and other renewable sources. The European market is mainly dominated by the production of bioethanol, with a predominance of diesel vehicles through a 60% share (80% estimated in the next 20 years) [1]. Therefore, the incorporation of bioethanol in diesel fuels may constitute an option to achieve the objective of 5.75% of biofuel share in transportation fuels by 2010 according to a European directive [2,3]. As bioethanol cannot be used directly in diesel fuel because of its non-miscibility with diesel blends, transformation processes must be considered.

The catalytic transformation of ethanol into higher added value products has been investigated for more than 3 decades [4–6]. Mixed oxides catalysts have been widely used allowing either the dehydrogenation of ethanol into acetaldehyde and acetals or higher alcohols, or its dehydration toward ethylene depending on the balance between acid and basic functions [7–10].

The synthesis of diethylacetal (1,1-diethoxyethane) from ethanol alone has been scarcely reported. It generally involves ethanol and acetaldehyde as starting materials [11–13]. The diethylacetal is known to be a good additive to diesel fuel blends [14–16], as well as an important starting chemical for the perfume industry and the synthesis of polyacetal resins [17,18]. The Guerbet condensation reaction of primary alcohols to form higher alcohols is an important industrial process [19,20]. However, the production of 1-butanol from ethanol over mixed oxides catalysts has seldom been investigated [21,22]. 1-Butanol, apart from being also an additive to gasoline [23], is an especially important building block for acrylic acid and acrylic esters as well as an extensively used solvent [8,24,25].

We report in this work the synthesis of Cu-Mg-Al-O mixed oxides with various compositions from layered double hydroxides (LDH) precursors and their catalytic activities in the conversion of ethanol. The reaction network leading to diethylacetal and 1-butanol as main products has been established. The influence of the experimental conditions and of the balance between the acidobasic and redox properties of the catalysts on the selectivities in diethylacetal and/or 1-butanol was also investigated.

2. Experimental

2.1. Catalysts preparation

LDH precursors were prepared by coprecipitation at constant pH (≈ 10) of suitable amounts of $\text{Mg}(\text{NO}_3)_2 \cdot 6\text{H}_2\text{O}$ and $\text{Al}(\text{NO}_3)_3 \cdot 9\text{H}_2\text{O}$ ($1 \leq \text{Mg/Al} \leq 5$) with a solution of NaOH (2 M) into a well-stirred

^{*} Corresponding author.

E-mail address: nathalie.tanchoux@enscm.fr (N. Tanchoux).

¹ Present address: Department of Technological Chemistry and Catalysis, University of Bucharest, 4-12, Blv. Regina Elisabeta, 030018 Bucharest, Romania.

Table 1
Textural properties of the samples.

Catalyst	Calcination temperature (K)	SA ^a (m ² g ⁻¹)	Pore volume (mL g ⁻¹)	Crystal size (nm)	Cu content (at.%)
CuO	823	004	–	–	–
MgAlO ₃	823	224	0.35	–	–
Cu ₁ MgAl ₍₃₎ O	823	189	0.28	–	01.1
Cu ₃ MgAl ₍₃₎ O	823	174 [175]	0.32	–	–
Cu ₅ MgAl ₍₃₎ O	823	180	0.23	–	06.7
Cu ₁₀ MgAl ₍₃₎ O	823	200	0.31	15	12.3
Cu ₂₀ MgAl ₍₃₎ O	823	140	0.26	28	22.9
Cu ₅ MgAl ₍₃₎ O	823	150	0.49	–	–
Cu ₅ MgAl ₍₃₎ O	823	182 [146 ^b]	0.32	–	–
Cu ₇ MgAl ₍₃₎ O	523	013	0.02	–	–
Cu ₇ MgAl ₍₃₎ O	623	222	0.31	–	–
Cu ₇ MgAl ₍₃₎ O	723	187	0.31	–	–
Cu ₇ MgAl ₍₃₎ O	823	176 [180]	0.32	–	–
Cu ₇ MgAl ₍₃₎ O	923	170	0.21	–	–

^a After reaction.

^b After 100 h reaction time.

beaker containing 200 mL of suitable amount of Cu(NO₃)₂·xH₂O (0.01 ≤ Cu/(Cu + Mg + Al) ≤ 0.2). The addition of the alkaline solution and the pH were controlled by pH-STAT Titrino (Metrohm). The precipitates formed were aged in their mother liquor overnight at 353 K under stirring, separated by centrifugation, washed with deionized water until a pH of 7 was reached and dried at 353 K overnight. The samples were noted Cu_xMgAl_(y)OH, where *x* is the copper content as atomic percent with respect to cations and *y* corresponds to the Mg/Al atomic ratio.

The previous dried samples were calcined in flowing nitrogen in the temperature range from 623 to 923 K (2 K min⁻¹) in order to obtain the corresponding mixed metal oxides catalysts (see Table 1). They were noted Cu_xMgAl_(y)O. The same method than that previously described, was used for preparing pure copper oxide.

2.2. Catalysts characterization

Powder X-ray diffraction (XRD) patterns were recorded using a Siemens D5000 Diffractometer and the monochromatic Cu-Kα1 radiation. They were recorded with 0.02° (2θ) steps over the 3–70° 2θ angular range with 1 s counting time per step.

The chemical composition of the samples was determined by EDX microprobe on a Cambridge Stereoscan 260 apparatus.

The textural characterization was achieved using conventional nitrogen adsorption/desorption method, with a Micromeritics ASAP 2010 automatic analyzer. Specific surface areas were calculated using the BET method. Prior to nitrogen adsorption, the samples were outgassed for 8 h at 523 K.

Temperature-programmed desorption (TPD) of CO₂ and NH₃ were carried out using a Micromeritics Autochem model 2910 instrument equipped with a programmable temperature furnace and a TCD detector. Fresh calcined samples (100 mg) were pretreated under air at 823 K before adsorption of the probe molecules at 373 K. During desorption, the sample was heated under a helium flow (30 mL/min) at a ramp of 10 K/min. The amount of probe molecules desorbed from the samples was calculated from the area under the peak corresponding to the TCD responses.

2.3. Catalytic test

The catalytic performances of the various catalysts were evaluated using 50 mL (39.5 g) of ethanol (Riedel-de Haën, 99.8%) in a 100 mL steel autoclave in the temperature range of 473–533 K and autogenic pressure under stirring. Unless specified, each run was carried out over a period of 5 h using 0.5 g of catalyst. The reaction products were analyzed by gas chromatography (HP

4890D, equipped with a DB-1 capillary column and a flame ionization detector), and the response factors related to decane as external standard were determined for ethanol and the products which were identified with pure commercial samples. The predominant reaction products were *n*-butanol, 1,1-diethoxyethane, acetaldehyde, ethyl acetate, butyraldehyde, 1,1-diethoxybutane, crotonaldehyde, methyl ethyl ketone and diethyl ether. The carbon and oxygen mass balances, based on the products listed, were always higher than 95%.

The conversion was calculated based on the number of carbon atoms observed in the reaction products as follows:

$$C(\%) = \frac{\sum_i n_i C_i}{2C_{\text{EtOH}} + \sum_i n_i C_i} \times 100$$

The selectivity for product *i* was calculated as follows:

$$S_i(\%) = \frac{n_i C_i}{\sum_i n_i C_i} \times 100$$

where *n_i* is number of carbon atoms in the product *i*; *C_i* is concentration of product *i* in the reaction products; *C_{EtOH}* is concentration of ethanol in the reaction products.

3. Results and discussion

3.1. Textural and structural properties of the catalysts

The XRD patterns of the as-prepared LDH precursors and of the catalysts obtained after calcination at 823 K are displayed in Figs. 1 and 2, respectively. The as-prepared samples exhibit the characteristic patterns of LDH with broad (0 0 3) and (0 0 6) diffraction peaks at ~10.50° and 21° 2θ. The corresponding interlayer distance *d*_{0 0 3} of ca. 8.40 Å is in agreement with the presence of nitrate anions in the interlayer space provided by the precursor salts [26]. For the samples with copper contents higher than 7%, we note the presence of tenorite. The formation of copper-side phases is often observed in the case of copper-containing hydrotalcites due to the Jahn–Teller effect in the Cu²⁺ ions [27]. Cu₅MgAl₍₁₎OH exhibits at ~20° and 40° 2θ the peaks of bayerite according to the high Al content of this sample. Cu₅MgAl₍₅₎OH displays the higher crystallinity and remarkably the interlayer distance slightly decreases to 8.07 Å. This accounts for the higher layer charge density of this sample.

After calcination at 823 K the catalysts exhibit the characteristic XRD patterns of the Mg(Al)O mixed oxide phase with the periclase structure. Tenorite with a rather similar crystallinity than the precursor is also detected for Cu loading higher than 7%. At lower loadings, Cu can form a solid solution with Mg and Al, or give well dispersed CuO crystallites not detected by XRD. The full-width at

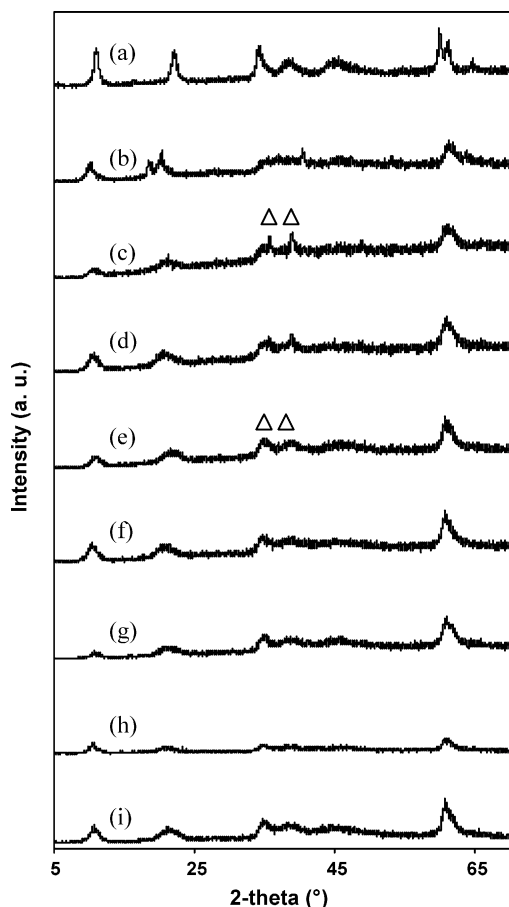


Fig. 1. XRD patterns of the LDH precursors. (a) $\text{Cu}_5\text{MgAl}_5(\text{OH})$; (b) $\text{Cu}_5\text{MgAl}_1(\text{OH})$; (c) $\text{Cu}_{20}\text{MgAl}_3(\text{OH})$; (d) $\text{Cu}_{10}\text{MgAl}_3(\text{OH})$; (e) $\text{Cu}_7\text{MgAl}_3(\text{OH})$; (f) $\text{Cu}_5\text{MgAl}_3(\text{OH})$; (g) $\text{Cu}_3\text{MgAl}_3(\text{OH})$; (h) $\text{Cu}_1\text{MgAl}_3(\text{OH})$; (i) $\text{MgAl}_3(\text{OH})$; (Δ) Tenorite phase.

half-maximum (FWHM) of the two most intense reflections of CuO in $\text{Cu}_{10}\text{MgAl}_3\text{O}$ and $\text{Cu}_{20}\text{MgAl}_3\text{O}$ catalysts allow to estimate the average crystallite size using the Debye–Scherrer equation. The crystallite size increases from 15 to 28 nm when the copper content in the catalyst increases from 10 to 20% (Table 1).

The copper content in the catalysts, determined by EDX, is slightly higher than the theoretical one, as shown in Table 1.

The textural properties of the catalysts in function of the composition and the temperature of treatment are also reported in Table 1. Besides the structural evolutions of $\text{Cu}_7\text{MgAl}_3\text{O}$ with the temperature followed by XRD are reported in Fig. 3. For the samples calcined at 823 K the specific surface areas are in the range of 225 to 170 $\text{m}^2 \text{g}^{-1}$ for Cu loadings up to 10% and decrease at 140 $\text{m}^2 \text{g}^{-1}$ when it reaches 20% due to the presence of CuO crystallites. $\text{Cu}_7\text{MgAl}_3\text{O}$ calcined at 523 K exhibits a very low specific surface area (13 $\text{m}^2 \text{g}^{-1}$) in agreement with its LDH structure. The structure moves to that of the poorly crystallized mixed oxide after calcination at 623 K and the specific surface area reaches its maximum value. It then decreases slightly from 220 to 170 $\text{m}^2 \text{g}^{-1}$ when the temperature increases up to 923 K due to the concurrent increase of crystallinity of the mixed oxide. All materials displayed type IV nitrogen adsorption/desorption isotherms with a hysteresis loop, characteristic of mesoporous materials. The absence of micropores in these materials was ascertained by the analysis of the t -plots derived from the sorption isotherms.

CO_2 -TPD profiles of the catalysts with a similar Mg/Al molar ratio of 3 and containing different amounts of copper are shown in Fig. 4. These very broad profiles extending from 373 to 773 K were

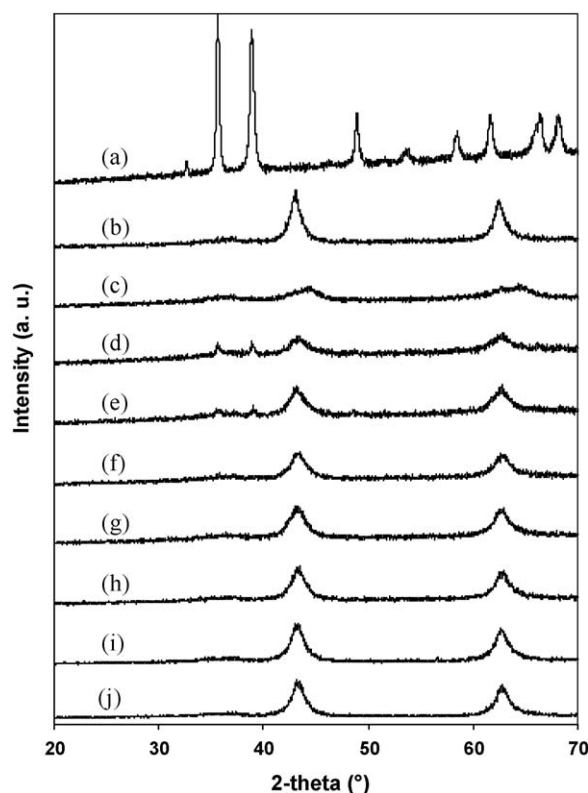


Fig. 2. XRD patterns of the catalysts calcined at 823 K: (a) CuO; (b) $\text{Cu}_5\text{MgAl}_5\text{O}$; (c) $\text{Cu}_5\text{MgAl}_1\text{O}$; (d) $\text{Cu}_{20}\text{MgAl}_3\text{O}$; (e) $\text{Cu}_{10}\text{MgAl}_3\text{O}$; (f) $\text{Cu}_7\text{MgAl}_3\text{O}$; (g) $\text{Cu}_5\text{MgAl}_3\text{O}$; (h) $\text{Cu}_3\text{MgAl}_3\text{O}$; (i) $\text{Cu}_1\text{MgAl}_3\text{O}$; (j) MgAl_3O .

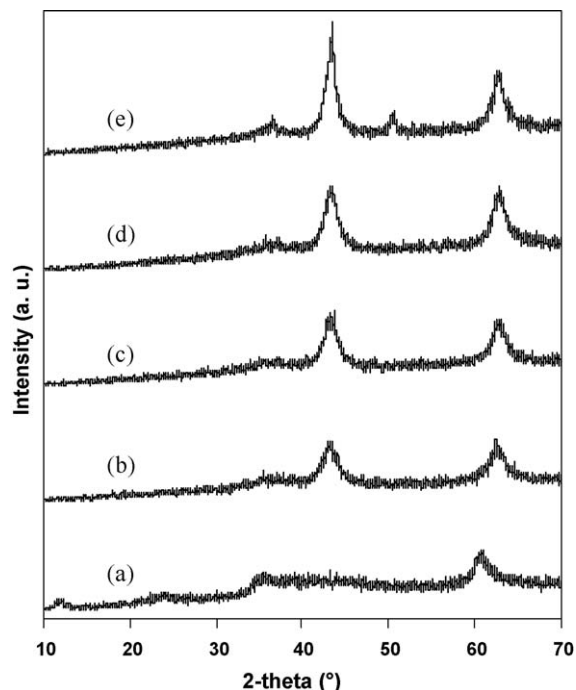


Fig. 3. XRD patterns of $\text{Cu}_7\text{MgAl}_3\text{O}$ calcined at: (a) 523 K; (b) 623 K; (c) 723 K; (d) 823 K; (e) 923 K.

deconvoluted in three desorption peaks with maxima at about 450, 500 and 575 K, accounting for the presence of sites of weak (W), moderate (M) and high (H) basic strength, respectively. The amount of CO_2 desorbed in these peaks allows to calculate the

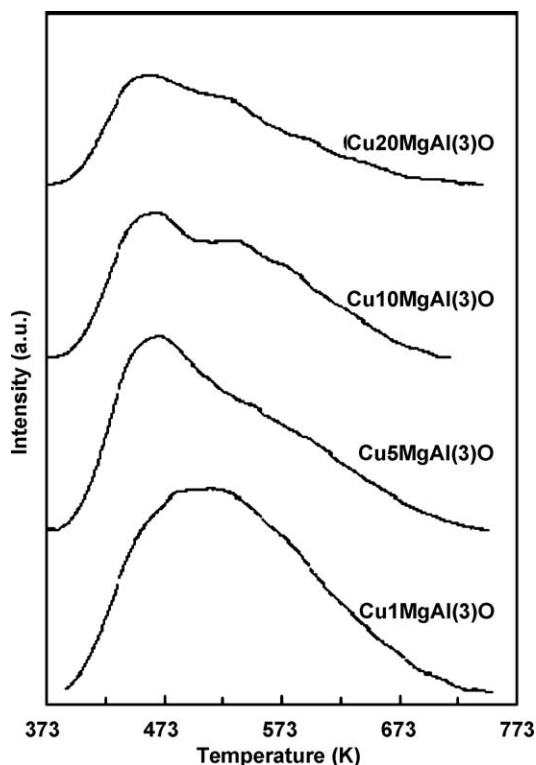


Fig. 4. CO₂-TPD profiles of: (a) Cu₁MgAl₍₃₎O; (b) Cu₅MgAl₍₃₎O; (c) Cu₁₀MgAl₍₃₎O; (d) Cu₂₀MgAl₍₃₎O.

number of sites reported in Table 2. The total number of basic sites decreases when the Cu content increases. This decrease concerns particularly the sites of medium and high strength.

NH₃-TPD profiles of the same catalysts are shown in Fig. 5. As in the case of the CO₂-TPD profiles, except for Cu₁MgAl₍₃₎O, they can be deconvoluted in three peaks with maxima at 454–462 K, 494–535 K and 569–631 K corresponding to acid sites exhibiting weak (W), moderate (M) and high strength (H), respectively. In the case of Cu₁MgAl₍₃₎O, the NH₃-TPD profile was deconvoluted only in two desorption peaks corresponding to sites with moderate and high acid strength. As already reported for CO₂, the number of sites was deduced from the area of each peak. The amount of each type of acid site is reported in Table 3. In contrast to the basic ones, there is

Table 2

Number of basic sites of different strength for CuMgAlO mixed oxides, derived from TPD of CO₂.

Catalyst	Number (mmol g ⁻¹)			Total number (mmol g ⁻¹)
	W	M	H	
Cu ₁ MgAl ₍₃₎ O	0.30	0.69	0.86	1.85
Cu ₅ MgAl ₍₃₎ O	0.37	0.42	0.79	1.58
Cu ₁₀ MgAl ₍₃₎ O	0.35	0.41	0.44	1.20
Cu ₂₀ MgAl ₍₃₎ O	0.23	0.33	0.33	0.89

Table 3

Number of acid sites of different strength for CuMgAlO mixed oxides, derived from TPD of NH₃.

Catalyst	Number (mmol g ⁻¹)			Total number (mmol g ⁻¹)
	W	M	H	
Cu ₁ MgAl ₍₃₎ O	–	1.30	0.64	1.94
Cu ₅ MgAl ₍₃₎ O	0.62	0.99	0.69	2.30
Cu ₁₀ MgAl ₍₃₎ O	0.23	0.89	0.34	1.46
Cu ₂₀ MgAl ₍₃₎ O	0.39	1.03	0.85	2.27

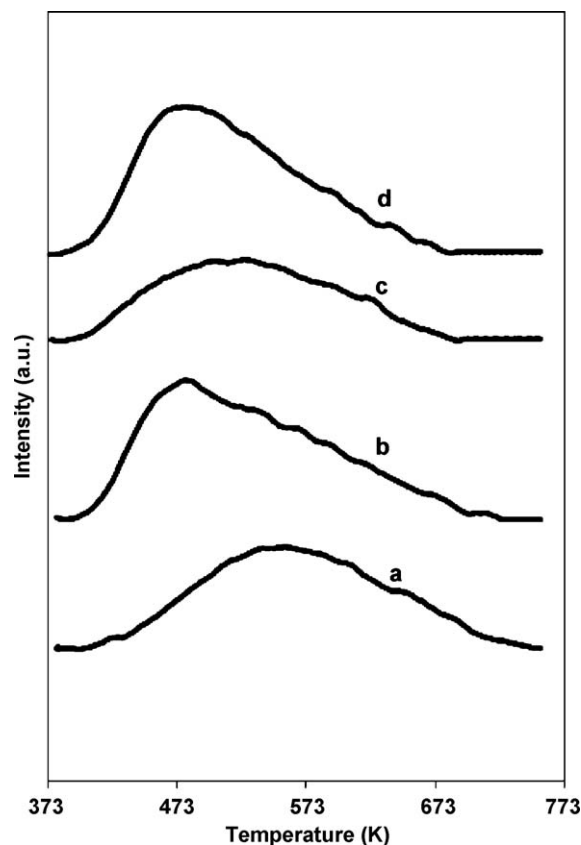


Fig. 5. NH₃-TPD profiles of: (a) Cu₁MgAl₍₃₎O; (b) Cu₅MgAl₍₃₎O; (c) Cu₁₀MgAl₍₃₎O; (d) Cu₂₀MgAl₍₃₎O.

no clear correlation between the number of acid sites of the samples and their copper content.

3.2. Catalytic study

Firstly, a blank experiment has been performed at 473 K during 5 h. As reported in Table 4, the conversion of ethanol was lower than 0.3% and the major product was 1,1-diethoxyethane. Trace amounts of acetaldehyde and diethyl ether were also observed. With MgAl₍₃₎O (Cu-free) catalyst, the conversion and selectivity are similar to those obtained for the blank test. When 5% of Cu is introduced in the catalyst Cu₅MgAl₍₃₎O, the conversion increased up to ~4% with selectivities of 40.3 and 35.9% into butanol and 1,1-diethoxyethane, respectively. 1,1-diethoxybutane, acetaldehyde, butyraldehyde, ethyl acetate and traces of crotonaldehyde were also observed among the reaction products.

A reaction scheme can be proposed for the reaction of ethanol on CuMgAlO catalysts in agreement with the nature of sites involved and the nature of the products obtained (Fig. 6). After the first step of ethanol dehydrogenation into acetaldehyde, two main pathways lead to: (i) 1-butanol by hydrogenation of butyraldehyde formed by self-condensation of acetaldehyde and (ii) 1,1-diethoxyethane by cross-condensation of ethanol and acetaldehyde.

Fig. 7 shows the effect of the Mg/Al ratio in the Cu₅MgAl_(y)O samples on the catalytic performances. The ethanol conversion remained practically unchanged at ~4% when the Mg/Al ratio was increased from 1 to 5. At the same time, the selectivity in butanol slightly decreased from 42 to 39.5%, while the selectivity in 1,1-diethoxyethane increased from 32 to 39%. The selectivities in minor products varied erratically but within a narrow range. These results show that the Mg/Al ratio does not influence the catalytic

Table 4Ethanol conversion and product selectivities in a blank test and over MgAl_2O_3 and $\text{Cu}_5\text{MgAl}_3\text{O}$ catalysts calcined at 823 K (5 h, 473 K).

Catalyst	Conversion (%)	Selectivities ^a (%)							
		Acetal C6	Acetal C8	Ethanal	Butanal	Crotonal	Butanol	EA	DET
Blank test	<0.300	86.1	–	7.3	–	–	–	–	6.5
MgAl_2O_3	0.3	87.5	–	6.1	–	–	–	–	6.3
$\text{Cu}_5\text{MgAl}_3\text{O}$	4.1	35.9	5.1	9.9	1.7	0.2	40.3	6.9	–

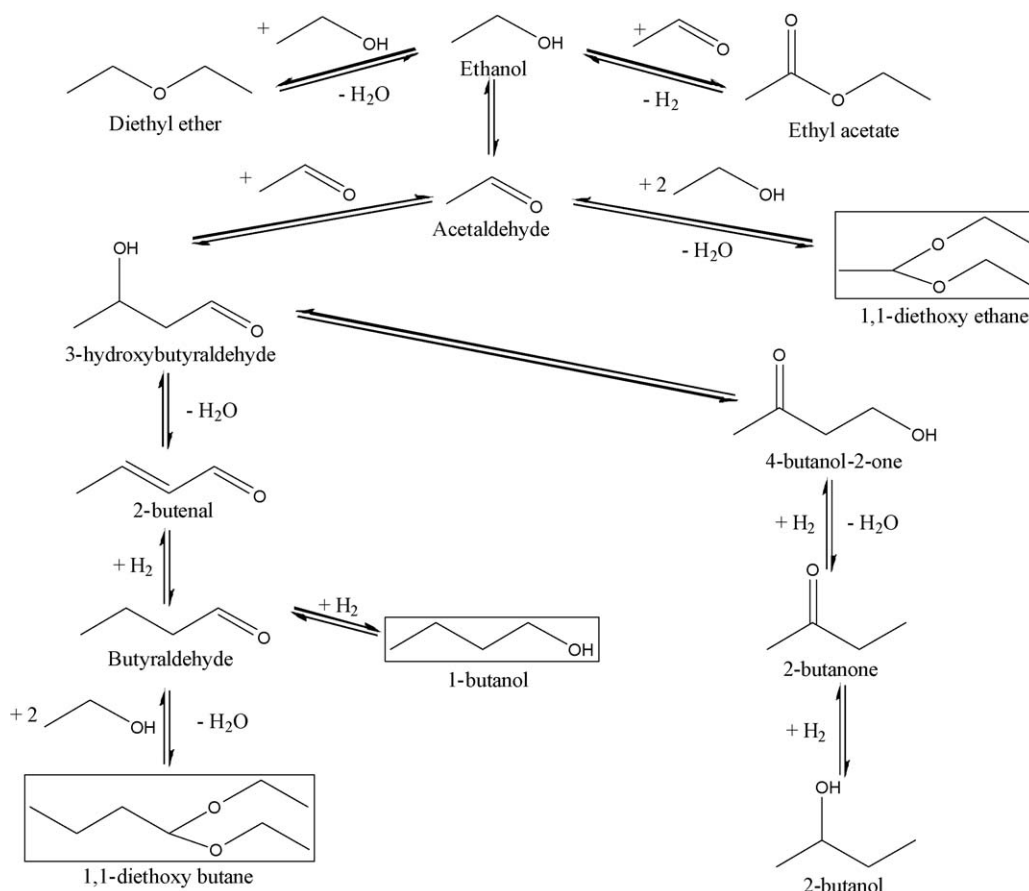
^a Acetal C6: 1,1-diethoxyethane; Acetal C8: 1,1-diethoxybutane; Ethanal: acetaldehyde; Butanal: butyraldehyde; Crotonal: crotonaldehyde; EA: ethyl acetate; DET: diethyl ether.

activity, and only slightly the selectivity. However, the different structural properties previously reported for this series of samples, particularly for $\text{Cu}_5\text{MgAl}_{(1)}\text{OH}$ and $\text{Cu}_5\text{MgAl}_{(5)}\text{OH}$ (Fig. 1), can hinder the influence of the Mg/Al ratio.

Fig. 8 shows the effect of the Cu content on the catalytic performances in the $\text{Cu}_x\text{MgAl}_{(3)}\text{O}$ samples. For the sake of comparison, the catalytic properties of CuO are also reported on Fig. 8. An optimum of conversion of 4.5% was observed for the catalyst with a 7% Cu content. This volcano shape can account for a decrease of the conversion due to a too low number of active sites below 7% of copper, and to the increase of the CuO average crystallite sizes above 7% (Table 1). Regarding the selectivities for the two main products of reaction, butanol and 1,1-diethoxyethane, they behave differently with increasing copper loading and the CuO crystal size. The selectivity for butanol indeed decreases regularly from ~42 to ~18%, while that of 1,1-diethoxyethane goes through a maximum value at 10% Cu. At high Cu content ($\text{Cu}_{20}\text{MgAl}_{(3)}\text{O}$) and for CuO, a marked decrease for both butanol and 1,1-diethoxyethane selectivities to the benefit of

ethyl acetate was observed. Moreover, in these cases, 2-butanol was also observed among the reaction products, the 1-butanol/2-butanol molar ratio being equal to 3.9 and 3.5 for $\text{Cu}_{20}\text{MgAl}_{(3)}\text{O}$ and CuO, respectively. We also note that the selectivity into ethyl acetate increased continuously with the copper content in the catalysts, becoming the main reaction product for $\text{Cu}_{20}\text{MgAl}_{(3)}\text{O}$ and CuO. The 1,1-diethoxybutane selectivity, always lower than 7%, decreased when the Cu content in the catalyst was increased, becoming almost zero for the CuO catalyst. The acetaldehyde and butyraldehyde selectivities varied irregularly as a function of the Cu content in the catalyst, between 3.2 and 11.7% and between 1.4 and 3.5%, respectively. We note that butyraldehyde was not observed on CuO. Traces of crotonaldehyde were observed only for the systems with Cu contents lower than 5%. XRD patterns of the catalysts after 5 h of reaction are similar to those before reaction (Fig. 9), therefore showing no structural evolution.

As previously underlined the acidity of the catalysts is not correlated to the copper content. Moreover, the catalytic properties are not correlated to their acidity. By contrast, a direct

**Fig. 6.** Reaction scheme for ethanol transformation on CuMgAlO catalysts. The targeted products are presented in a frame.

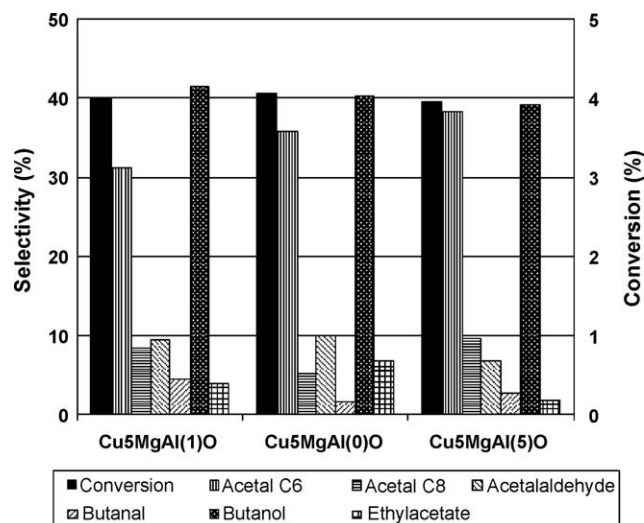


Fig. 7. Influence of the Mg/Al ratio on the catalytic activity of the $\text{Cu}_5\text{MgAl}(\gamma)\text{O}$ samples ($\gamma = 1, 3$ and 5) (5 h, 473 K).

relationship was evidenced between the basicity of these catalysts and the selectivity for *n*-butanol: the selectivity for *n*-butanol increased when the number of strong basic sites increased, as shown in Fig. 10. No relationship was found between basicity and 1,1-diethoxyethane selectivity. This suggests that acetaldehyde self-condensation would be the rate determining step of the reaction leading to *n*-butanol. Moreover, this reaction probably involves stronger basic sites than those required for the condensation between acetaldehyde and ethanol leading to 1,1-diethoxyethane.

The effect of the calcination temperature of the LDH precursors on the catalytic properties was studied using $\text{Cu}_7\text{MgAl}(\text{O})$. The results are presented in Fig. 11. Up to 623 K the conversion remained lower than 1%. It must be noted that, as already shown, the catalyst is in the lamellar form in this case. The conversion then increased with the calcination temperature. The maximum was reached at 823 K, the catalyst being in the mixed oxide form. The selectivities for butanol and 1,1-diethoxyethane showed opposite behaviors, the former increasing regularly with the calcinations

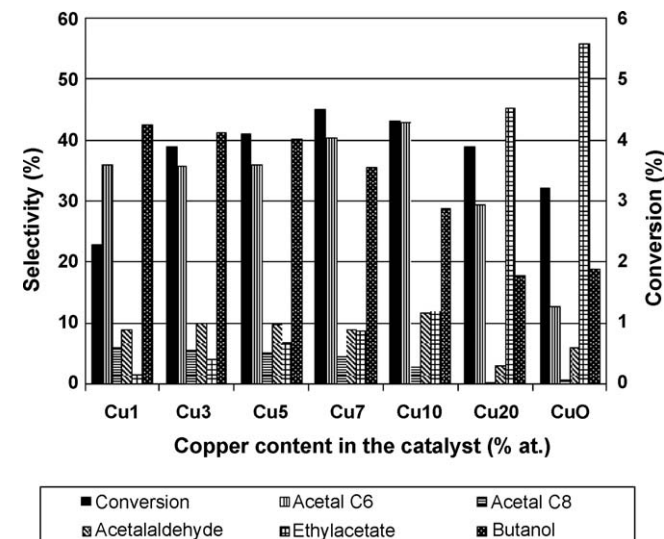


Fig. 8. Influence of the Cu content on the catalytic activity of the $\text{Cu}_x\text{MgAl}(\text{O})$ samples (5 h, 473 K).

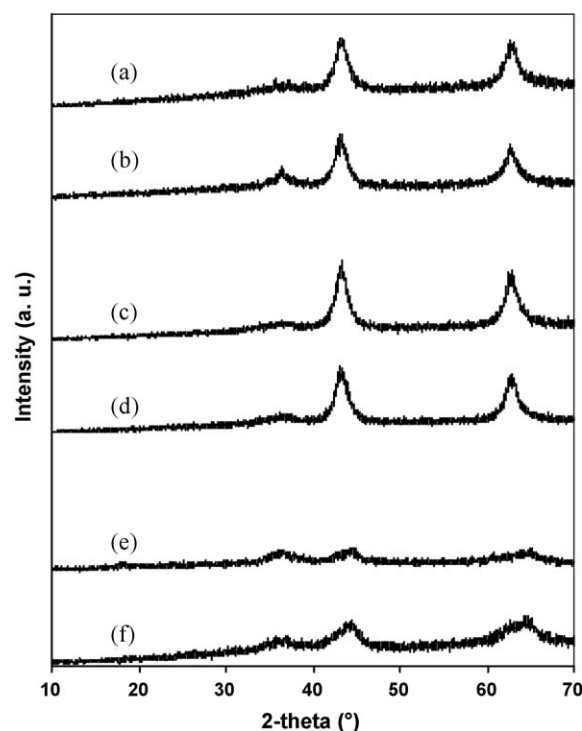


Fig. 9. XRD patterns of the catalysts before and after the catalytic test (5 h, 473 K) (a) fresh $\text{Cu}_7\text{MgAl}(\text{O})$; (b) $\text{Cu}_7\text{MgAl}(\text{O})$ after test; (c) fresh $\text{Cu}_3\text{MgAl}(\text{O})$; (d) $\text{Cu}_3\text{MgAl}(\text{O})$ after test; (e) fresh $\text{Cu}_5\text{MgAl}(\text{O})$; (f) $\text{Cu}_5\text{MgAl}(\text{O})$ after test.

temperature. The highest butanol yields were obtained for calcination temperatures above 723 K. We note that with the catalyst calcined at 923 K, methyl ethyl ketone was observed among the reaction products.

We checked the stability of the catalyst by carrying out the reaction with $\text{Cu}_7\text{MgAl}(\text{O})$ calcined at 823 K, three times successively. Between each reaction the catalyst was recovered by filtration and dried overnight at 523 K. The results obtained are shown in Fig. 12. The conversion remained almost similar in each run and only minor changes of selectivities were observed. It can be considered that the catalytic properties are maintained after three successive reactions.

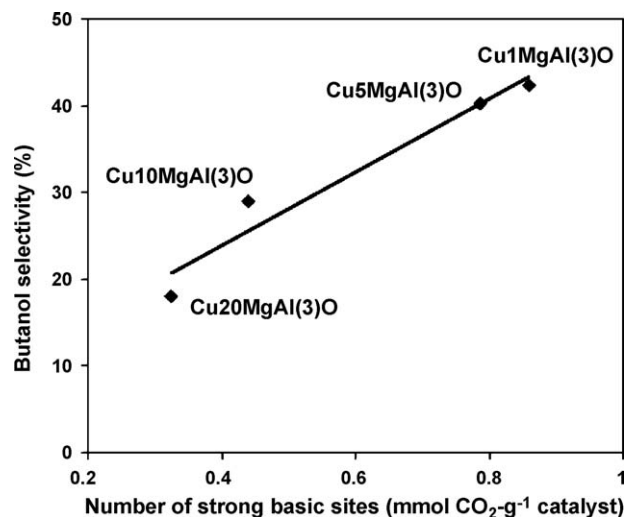


Fig. 10. Selectivity for *n*-butanol versus the number of strong basic sites.

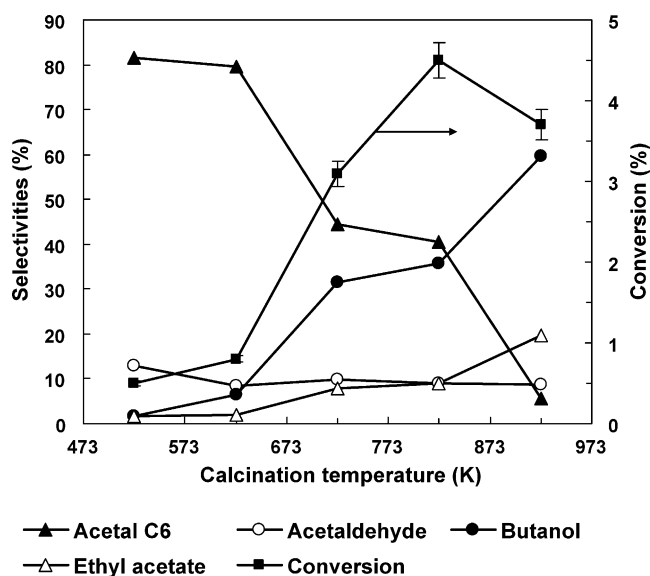


Fig. 11. Influence of the calcination temperature of the LDH precursor on the catalytic properties of $\text{Cu}_7\text{MgAl}_3\text{O}$.

Fig. 13 shows the variations of conversion and selectivities with the reaction temperature in the range 473–533 K for the $\text{Cu}_5\text{MgAl}_5\text{O}$ catalyst. As expected, the conversion increased with the reaction temperature from ~4% at 473 K to ~9% at 533 K. At the same time, the selectivity for butanol increased up to 80% at the expense of acetals. These results may be compared with those reported by Ndou et al. [22] where the best selectivity for butanol was ~18% for an ethanol conversion of ~56% at 723 K.

When the reaction is performed at 473 K and the reaction time increased from 2 to 100 h, the conversion increased from 2.6 to 11.1% and the selectivity for butanol reached 67.6% (Fig. 14) while that for 1,1-diethoxyethane decreased.

It is well-known that, in the case of mixed oxides obtained from hydrotalcite precursors, water can have a specific influence [28,29]. Therefore, the influence of the addition of water, as well as its removal from the reaction medium, was also studied (see Table 5).

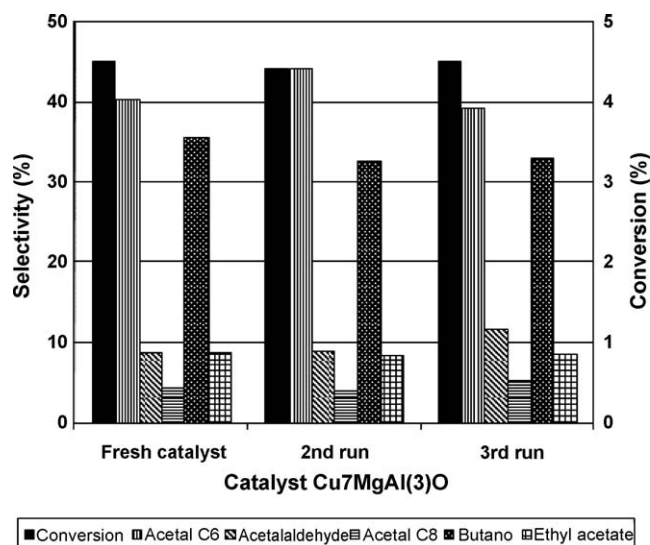


Fig. 12. Reusability of $\text{Cu}_7\text{MgAl}_3\text{O}$ (5 h, 473 K).

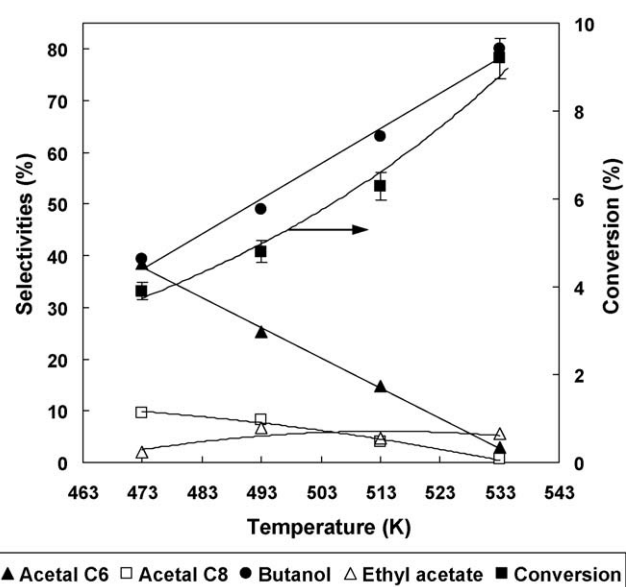


Fig. 13. Variation of the total conversion of ethanol and of the selectivities as a function of the reaction temperature for $\text{Cu}_5\text{MgAl}_5\text{O}$ (5 h).

The addition of water to the reaction mixture, which is also a by-product of the reaction (see Fig. 6), has a negative effect on the catalytic activity (Table 5), as expected from the reversibility of all the processes involved. The selectivity into acetaldehyde, a primary dehydrogenation product, and 1,1-diethoxyethane increased in the presence of water, while that into butanol dramatically decreased in all cases studied. This is in agreement with the transformation of the Lewis strong basic sites O^{2-} into weaker Brønsted OH^- sites due to the presence of water.

An attempt was also made to remove water from the reaction medium to try to displace the equilibria and push the conversion further.

After a typical test, the reaction mixture, separated by filtration, was dried using MgSO_4 treated at 523 K overnight under N_2 , and after a new separation by filtration, re-engaged in the autoclave in the presence of a fresh catalyst load for a new run. A significant increase of the conversion accompanied by an increase of the selectivity for butanol and a decrease of the selectivity for 1,1-

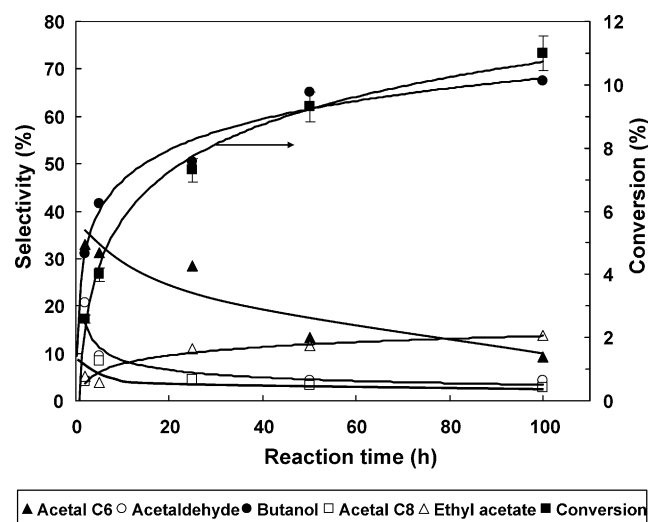


Fig. 14. Effect of the reaction time on the catalytic properties of $\text{Cu}_5\text{MgAl}_1\text{O}$ (473 K).

Table 5Influence of water on the catalytic properties of CuMgAlO mixed oxides ($T = 473$ K).

Catalyst	Solvent	t (h)	Conversion (%)	Selectivities ^a (%)						
				Acetal C6	Acetal C8	Ethanal	Butanal	Crotonal	Butanol	EA
Cu ₁ MgAl ₍₃₎ O	Ethanol	5	2.3	36.0	6.0	9.0	3.0	1.7	42.4	1.8
Cu ₁ MgAl ₍₃₎ O	Ethanol 96%	5	0.5	53.5	–	46.5	–	–	–	–
Cu ₅ MgAl ₍₁₎ O	Ethanol	25	7.3	28.4	4.6	4.6	0.8	–	50.5	10.9
Cu ₅ MgAl ₍₁₎ O	Ethanol 96%	25	1.5	36.8	2.7	36.8	4.1	5.2	3.8	10.8
Cu ₇ MgAl ₍₃₎ O	Ethanol	5	4.5	40.5	4.6	9.0	1.4	–	35.6	8.9
Cu ₇ MgAl ₍₃₎ O	Ethanol ^b	5	7.2	24.9	3.5	15.3	3.7	0.5	47.4	8.7

^a Acetal C6: 1,1-diethoxyethane; Acetal C8: 1,1-diethoxybutane; Ethanal: acetaldehyde; Butanal: butyraldehyde; Crotonal: crotonaldehyde; EA: ethyl acetate; DET: diethyl ether.

^b New run with a fresh catalysts after drying on MgSO₄.

diethoxyethane was observed. These results are in accordance with the preservation of Lewis stronger basic sites O²⁻ due to the removal of water.

4. Conclusion

Ethanol conversion into butanol and acetal is possible over CuMgAlO mixed oxide catalysts. The orientation of the transformation towards one or another main product depends on the reaction conditions and on the composition of mixed oxides, mainly the copper content. The reaction is oriented towards butanol at higher reaction temperatures or at longer reaction times. At 473 K the ethanol conversion amounted to ~11% when the reaction time was set at 100 h. At the same time the selectivity for butanol was increased to ~70%. The ethanol conversion and the selectivity for butanol reached ~9 and ~80%, respectively, when the reaction temperature was set at 533 K.

Calcination of the precursor at 823 K gives a material characterized by an optimum of catalytic activity.

Contrarily to the Mg/Al ratio, which does not play a very important role on the catalytic properties of the studied catalysts, the copper content proves very important. An optimum for the Cu contents in the CuMgAlO mixed oxides between 5 and 10 at.% with respect to the cationic species was observed. Over catalysts with high loadings in copper or pure copper oxide, the main pathway is the condensation of ethanol with acetaldehyde resulting in ethyl acetate formation. The strong and the total basicities of the catalysts decreased with increasing the copper content and the selectivity for *n*-butanol increased when the number of strong basic sites increased.

The structural and textural features of the catalysts used in 5 h catalytic runs remained unchanged. When the reaction time was increased to 100 h, the conversion and the selectivity for butanol increase.

The presence of water in the reaction mixture (either produced by the reaction or added with the feed) has a negative effect on the catalytic activity of the catalysts. Further experiments will be designed with the aim of continuously removing water from the reaction medium and will be reported in a near future.

Acknowledgements

The authors are grateful to Mr. Thomas Cacciaguerra for his expert technical assistance with EDX analysis and XRD spectra recording. This work was performed within the frame of ANR BioEdiesel number ANR-06-BLAN-0005.

References

- [1] D. Ballerini, Les biocarburants. Editions Technip, IFP Publications, 2006.
- [2] Actes du Colloque National: "De l'or noir à l'or vert? L'avenir industriel des bioproduits", AGRICE, 9 Novembre 2004.
- [3] Directive 2003/30/EC of the European Parliament, EN Official Journal of the European Union L123 (2003) 44.
- [4] J. Frankaerts, G.F. Froment, Chem. Eng. Sci. 19 (1964) 807.
- [5] A. Pelso, M. Moresi, C. Mustachi, B. Soracco, Can. J. Chem. Eng. 57 (1979) 159.
- [6] J. Edwards, J. Nicolaidis, M.B. Cultrip, C.O. Bennett, J. Catal. 50 (1977) 24.
- [7] E. Iglesia, D.G. Barton, J.A. Biscardi, M.J.L. Gines, S.L. Soled, Catal. Today 38 (1997) 339.
- [8] M.J.L. Gines, E. Iglesia, J. Catal. 176 (1998) 155.
- [9] J.I. Cosimo, V.K. Diez, M. Xu, E. Iglesia, C.R. Apesteguia, J. Catal. 178 (1998) 499.
- [10] H. Hattori, Chem. Rev. 95 (1995) 537.
- [11] P.L. Bramwyche, M. Mugdan, H.M. Stanley, Distillers Co. Ltd., US Patent 2,519,540 (1950).
- [12] V.M.T.M. Silva, A.E. Rodrigues, Chem. Eng. Sci. 56 (2001) 1255.
- [13] M.F. Gomez, L.A. Arrua, M.C. Abello, React. Kinet. Catal. Lett. 73 (2001) 143.
- [14] M. Natarajan, E.A. Frame, T. Asmus, W. Clark, J. Garbak, M.A. Gonzalez, E. Liney, W. Piel, J.P. Wallace III, SAE Tech. Pap. Ser., 2001, 2001-01-3631.
- [15] B.E. Hallgren, J.B. Heywood, SAE Tech. Pap. Ser., 2001, 2001-01-0648.
- [16] A.S. Cheng, R.W. Dibble, B.A. Buchholz, SAE Tech. Pap. Ser., 2002, 2002-01-1705.
- [17] M. Kauffhold, M. El-Chabawi, Huels Chemische Werke AG, US Patent 5,527,969 (1996).
- [18] T. Aizawa, H. Nakamura, K. Wakabayashi, T. Kudo, H. Hasegawa, Showa Denko KK, US Patent 5,362,918 (1994).
- [19] M.W. Farrar, Monsanto Chemical Co., US Patent 2,971,033 (1961).
- [20] R.T. Clark, Celanese Corporation, US Patent 3,972,952 (1976).
- [21] C. Yang, Z. Meng, J. Catal. 142 (1993) 37.
- [22] A.S. Ndou, N. Plint, N.J. Coville, Appl. Catal. A: Gen. 251 (2003) 337.
- [23] R.E. Kirk, D.F. Othmer, third ed., Encyclopedia of Chemical Technology, vol. 4, 1978, p. 338.
- [24] A.M. Hilmen, M. Xu, M.J.L. Gines, E. Iglesia, Appl. Catal. A: Gen. 169 (1998) 355.
- [25] J.I. Di Cosimo, C.R. Apesteguia, M.J.L. Gines, E. Iglesia, J. Catal. 190 (2000) 261.
- [26] V. Rives, M.A. Ulibarri, Coord. Chem. Rev. 181 (1999) 61.
- [27] A. Alejandre, F. Medina, P. Salagre, X. Correig, J.E. Sueiras, Chem. Mater. 11 (1999) 939.
- [28] S. Abelló, F. Medina, X. Rodríguez, Y. Cesteros, P. Salagre, J.E. Sueiras, D. Tichit, B. Coq, Chem. Commun. (2004) 1096.
- [29] S. Abelló, F. Medina, D. Tichit, J. Pérez-Ramírez, J.C. Groen, J.E. Sueiras, P. Salagre, Y. Cesteros, Chem. Eur. J. 11 (2005) 728.